PCCP

Femtosecond concerted elimination of halogen molecules from halogenated alkanes

Una Marvet,† Emily J. Brown and Marcos Dantus*

Department of Chemistry and Center for Fundamental Materials Research, Michigan State University, E. Lansing, MI 48824-1322, USA. E-mail: dantus@cem.msu.edu

Received 12th October 1999, Accepted 21st December 1999

The concerted dynamics involved in the molecular detachment of halogenated alkanes, *i.e.*, $CX_2YZ \rightarrow CX_2 + YZ$ (where X = H, F or Cl and Y, Z = I, Br or Cl) have been studied by femtosecond pump–probe spectroscopy. Particular emphasis has been placed on exploring the role of symmetry in the parent molecule. For experiments carried out on CH_2ICl, product fluorescence was observed in two regions of the spectrum: at 430 nm, corresponding to the $D' \rightarrow A'$ transition, and at 340 nm, attributed to the $G \rightarrow A$ transition. Differences in the dissociation time for the two pathways can be understood by considering the energy available for fragment recoil. The elimination process was found to be slower for methylene bromide than for methylene iodide, possibly because of the difference in the enthalpy of reaction. When three gem-dibromo compounds (Y, Z = Br, X = H, F or Cl) were compared, they were found to have significantly different dissociation times: 29.7 fs for the fluorinated species, 58.6 fs for the hydrogenated species, and 80.6 fs for the chlorinated species. The difference in the transition state lifetime between the hydrogenated and chlorinated species can be rationalized in terms of changes in the reduced mass, the thermodynamics of the reactions, and the energy partitioning. The fluorinated compound was found to dissociate much faster than predicted by thermodynamic and reduced mass arguments.

Introduction

In recent years, a number of groups have addressed the dynamics involved in the formation of halogen molecules following high-energy excitation of halogenated alkanes.[1–16] Previous papers from our group have examined the concerted mechanism of this process.[9–15] When methylene iodide (CH_2I_2) is the parent molecule, high-energy excitation produces molecular iodine. Coherent vibrational motion in the I_2 product was observed.[10] Analysis of the transition state dynamics shows that the carbon–halogen bonds are broken and the interhalogen bond formed within 50 fs of the initial excitation. The dissociation dynamics of CH_2I_2 and gem-diiodobutane (BuI_2) were compared; the transition state lifetime for BuI_2 is approximately twice that of CH_2I_2. Analysis based on a reduced mass argument indicated that the reaction occurred faster than intramolecular vibrational relaxation (IVR).[11,13] In this study, we use the mixed halogen compound CH_2ICl to explore the role of symmetry in the concerted elimination process. The dynamics observed for the photodetachment process of methylene bromide are examined and an analysis is made of the effects of exchanging fluorine or chlorine for the hydrogen atoms in this family of compounds. These substitutions result in large changes in the center of mass and in bond strengths.

Earlier work from our group investigated photolysis of CH_2I_2 to produce $CH_2 + I_2(D')$[10,11,13] using a three-photon excitation with a total energy of 12 eV. This reaction channel was first investigated by Style and coworkers[1,2] and later by Okabe and coworkers.[5] More recently we have compared these results with the dynamics of a less favored dissociation channel with the same 12 eV excitation leading to CH_2 and $I_2(f)$.[14,15] Unlike the earlier studies on the $CH_2 + I_2(D')$ channel, the $CH_2 + I_2(f)$ dynamics showed very clear rotational anisotropy. This rotational component of the data allowed a much clearer picture of the mechanism involved in this dissociation process. Analysis of the rotational anisotropy indicated that $I_2(f)$ is produced with a very hot rotational distribution. It is apparent from classical mechanical modeling of the dynamics that the symmetry of the molecule must be broken during dissociation in order to achieve this kind of distribution. An asynchronous concerted process does not conserve the C_{2v} symmetry and is consistent with the observed dynamics. A synchronous concerted mechanism in which the C_{2v} symmetry of the parent is conserved would produce rotationally cold products (see Fig. 1b).

Fig. 1c depicts the 'stepwise' (non-concerted) pathways producing I and I*. These reaction channels dominate the photodissociation. Although the energy required for the production of ground-state molecular iodine from gem-diiodomethane is quite modest (30 000 cm^{-1}), molecular iodine has only been detected when the excitation wavelengths have been shorter than 200 nm, corresponding to an excitation energy of 50 000 cm^{-1}.[1,2,4–6,8] Even at high excitation energies, the yield for molecular detachment processes remains below 1%. To explain the low yield of molecular products, Kawasaki *et al.* have invoked the existence of a barrier that prevents molecular detachment from the lower energy states because of symmetry considerations.[3] Cain *et al.* have performed calculations based on a generic gem-dihalogenated compound and confirmed the existence of the barrier.[7] In their work they proposed a mechanism in which the halogen molecule twists as it leaves the carbene fragment. This process corresponds to the asynchronous mechanism shown in Fig. 1b. We have addressed the subject of molecular elimination from

† Current address: University of Toronto, Department of Chemistry, 80 St. George Street, Toronto, Ontario, Canada M5S 3H6.

DOI: 10.1039/a908173i

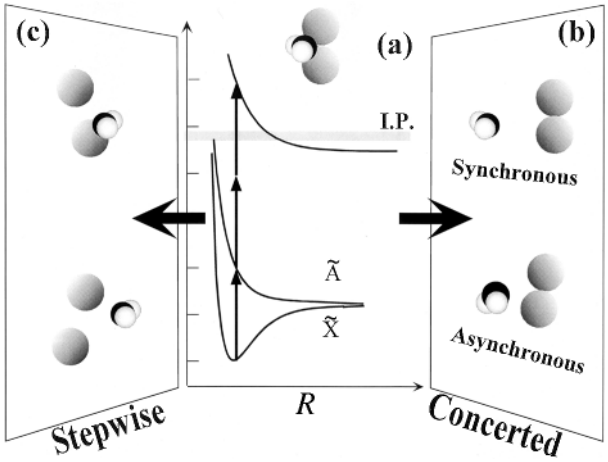

Fig. 1 (a) Schematics of the relevant potential energy surfaces involved in the multiphoton excitation of CX_2Y_2. Following the absorption of the photons, multiple pathways are available for the photodetachment process. The molecule can dissociate in a concerted process (producing $CX_2 + Y_2$) or a stepwise process (producing $CX_2 + 2Y$ or $CX_2Y + Y$). (b) In the concerted mechanism, the molecule can either maintain C_{2v} symmetry during the dissociation process (synchronous) leading to a small rotational excitation or break the C_{2v} symmetry (asynchronous) resulting in a high rotational distribution. In either case, coherent vibration of halogen molecule would be obtained. (c) In the stepwise mechanism, the molecular halogen is not formed within the vibrational period of the molecule; thus, coherent vibration of the halogen molecule would not be obtained.

CH_2I_2 taking into account the role of symmetry in preventing the observation of this channel at low excitation energies (<5 eV).[11,13] From this analysis, it became clear that the amount of internal energy in the halogen product, following high energy excitation, would be sufficient to dissociate the lower valence states.[11,13] Ion pair states correlating with $X^+ + X^-$ are strongly bound and therefore are the best candidates for surviving the high internal energy deposited in the products. The findings reported in this study are consistent with this general understanding even for mixed halogen compounds.

Huber and coworkers have studied the dissociation pathways of CF_2I_2 by excitation at wavelengths between 248 and 351 nm. Their findings indicate that production of I and I* constitute the major dissociation channels for the reaction.[17–19] Huber, Radloff, and coworkers studied the dissociation pathways of CF_2I_2 with ultrafast laser pulses. As with diiodomethane, difluorodiiodomethane produces I_2 following high-energy excitation; in this case, the reaction is initiated by absorption of two photons at 267 nm.[16] This study did not identify the electronic state of the molecular halogen nor its vibrational or rotational energetics. Schwartz *et al.* have studied the photodissociation dynamics of CH_2I_2 with femtosecond lasers in a variety of solvents.[20] Their work focused on the reaction initiated by the 310 nm pump and producing $CH_2I + I$. They followed the geminate recombination of the photoproducts by measuring transient absorption at 620 nm and found that the primary geminate recombination occurred on a $\sim$350 fs time scale. Tarnovsky *et al.* studied the photodissociation dynamics of CH_2I_2 in acetonitrile by femtosecond pump–probe spectroscopy.[21] Their data, following a 310 nm pump pulse and probing with wavelengths 240–1220 nm, reproduced the initial 350 fs decay. The wide range of probe wavelengths allowed them to estimate the rate of cooling of the CH_2I photoproduct (5–8 ps) and revealed the formation of the CH_2I–I, an ion-pair isomer of CH_2I_2. Isodiiodomethane, CH_2I–I, has been observed in noble gas matrices at low excitation energies.[22] The initial dynamics that take place upon excitation of CH_2I_2 have been studied by Kiefer and coworkers (gas phase) and by Kwok and Phillips (in solution) between 342 and 369 nm by resonance Raman scattering.[23–25] Their findings indicate the involvement of the I–C–I symmetric stretch, asymmetric stretch and bending vibrational modes.

This paper is organized as follows. The Experimental section briefly describes the laser system used to obtain the measurements presented here. The section on Results and discussion provides experimental data collected to investigate various aspects of photoinduced molecular detachment. Experiments on CH_2ICl allow us to explore the preferred molecular detachment pathway for a molecule without C_{2v} symmetry. The dissociation dynamics of CH_2I_2 and CH_2Br_2 are compared and analyzed with respect to the reduced mass and reaction enthalpies. Lastly, we observe differences in the transition state lifetimes for the family of compounds CX_2Br_2, where X is H, F or Cl. The final section draws conclusions based on our observations.

Experimental

The experimental setup for these measurements has been described previously.[13] The reaction is initiated by multiphoton excitation of the parent molecule using a 312 nm pump pulse. Fluorescence spectra of the product molecules were measured by dispersion with a 0.27 m spectrometer. The time-resolved data (transients) were obtained by fluorescence depletion caused by the 624 nm probe pulse, measured as a function of pump–probe time delay. Rotational anisotropy measurements were obtained by measuring the time-dependent data with the polarization of the probe laser parallel or perpendicular to the polarization of the pump laser. The intensity of the probe beam was attenuated such that the probe pulse alone did not produce any detectable fluorescence. The appropriate alkyl halide, all obtained from Aldrich with purity exceeding 95%, was placed in a static quartz cell and the temperature controlled such that the vapor pressure was maintained in the range 0.1–10 Torr. This pressure range ensured that no significant collisional relaxation occurred within the fluorescence lifetime of the halogen product states (typically $\sim$10 ns). Copper wire and sodium thiosulfate crystals were added to the cells to scavenge any halogen molecules that may be present in the sample.

Results and discussion

A. Dissociation dynamics of CH_2ICl: breaking the C_{2v} symmetry

Previous studies on CH_2I_2 showed that the dissociation process that produces $CH_2 + I_2(f)$ follows a mechanism in which the C_{2v} symmetry is not maintained.[14,15] To explore the photodetachment process in a molecule without C_{2v} symmetry, experiments were conducted on gas-phase CH_2ICl (at 0 °C). Time-dependent data were observed from this molecule at two wavelengths, 340 nm and 430 nm. The 430 nm fluorescence can be assigned to the $D' \rightarrow A'$ transition of ICl.[26,27] The fluorescence between 325 and 340 nm has been tentatively assigned to the $G(^3P_1) \rightarrow A(^3\Pi_1)$ transition of ICl.[28]

It is known that ICl decomposes readily to produce I_2.[29] Therefore, spectra from neat I_2 vapor and from the CH_2ICl sample were compared to ensure that the signal at 340 nm was due to ICl not I_2 (see Fig. 2a). We assign the signal to ICl and not to I_2 for a number of reasons. (a) The experimental cell was kept at 0 °C. At this temperature the vapour pressure of I_2 is $\sim$0.06 Torr,[30,31] much smaller than the pressure in the neat I_2 cell $\sim$0.3 Torr. (b) The presence of halogen scavenging agents prevents the accumulation of I_2 or ICl. (c) There are clear spectroscopic differences between ICl and I_2 fluorescence (see Fig. 2a and 2b). (d) Spectral comparisons also indicate that I_2 fluorescence does not contribute significantly to the fluorescence at 430 nm (see Fig. 2b). (e) Furthermore, any contamination in the time-dependent data from I_2 molecules would only be observed at negative time delays where the 624

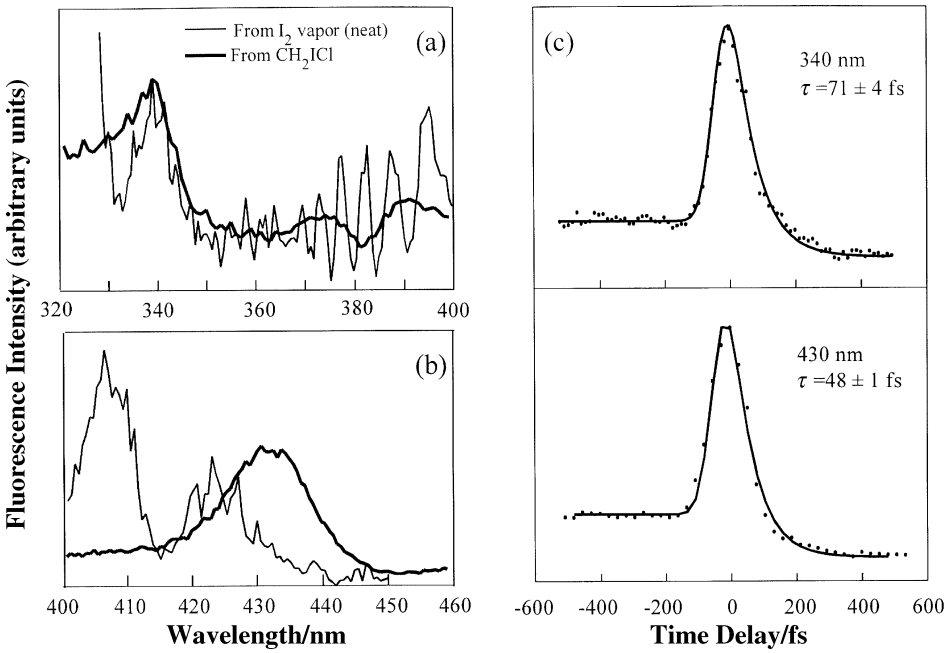

Fig. 2 Spectra from the CH_2ICl cell at 0 °C and an I_2 vapor cell, collected under 310 nm excitation, showing fluorescence in (a) the 320–400 nm region and (b) the 400–460 nm region. (c) Upper: experimental pump–probe data (dots) from the photoinduced dissociation of CH_2ICl detected at 340 nm. The fluorescence at this wavelength corresponds to the G → A transition in ICl. The displayed fit (line) corresponds to a transition state lifetime of 71 ± 4 fs. Lower: same as above except detected at 430 nm, assigned to the D′ → A′ transition in ICl. The dissociation time for this photodetachment process is 48 ± 1 fs.

nm pulse is the pump and the 312 nm pulse is the probe.[10] This contribution, if present at all, would not affect the results observed for positive time delays. Based on these observations, we conclude that the source of the signal in these experiments is ICl fluorescence.

The pump–probe data collected at these two wavelengths from the CH_2ICl cell at 0 °C are displayed in Fig. 2c. In both cases, an intense time zero enhancement and fluorescence depletion at positive pump–probe time delays are observed in the signal. Fits of the transition state lifetimes for the CH_2ICl dissociation (for each product channel) are also shown in Fig. 2c. These fits were obtained using the fitting method outlined by Marvet *et al.*[13] and yielded $1/e$ times of 71 ± 4 fs (G state) and 48 ± 1 fs (D′ state). Previously, the transition state lifetime of the analogous process in CH_2I_2 (producing I_2 in the D′ state) was determined to be 47 ± 3 fs.[13] The uncertainty values obtained from the fitting routine are based on the assumption that the pulse duration of the laser is known exactly. Realistically, a ±10 fs confidence level should be included due to the uncertainties in the determination of the temporal response of our system resulting from the cross-correlation of the pump and probe lasers and noise in the data. In order to understand the difference in the lifetime for these two compounds, we need to examine the relationship between the reduced mass of the fragments and the energy available for recoil in each process.

Zewail and coworkers introduced a classical model to relate transition state lifetimes and the energy available after dissociation.[32,33] The dissociation time ($\tau_{1/2}$) is given as

$$\tau_{1/2} = \frac{L_1}{v} \ln\left(\frac{4E}{\gamma}\right). \quad (1)$$

where v is the terminal velocity of the fragments and γ the spectral width of the probe pulse. L_1 represents the length parameter of the potential and E is the energy available for recoil. Given the fact that the potential energy surfaces are not known for the compounds being studied, absolute numbers can not be calculated. It seems reasonable to assume that L_1 is similar, within an order of magnitude, for the molecules studied here based on relative bond strengths, molecular geometry, the speed of the detachment mechanism, and the large amounts of excess energy. Therefore, we assume the potentials to be similar within this family of CX_2YZ compounds (where X = H, F, or Cl and Y, Z = Cl, Br, or I) allowing us to compare the transition state lifetimes among these compounds. Furthermore, in comparing results one can assume that the time taken for dissociating fragments to achieve terminal velocity is proportional to their reduced mass.

The resulting impulsive model assumes that the parent molecule is a pseudodiatomic, breaking into the carbene radical and the halogen molecule, and that the fragments reach terminal velocity immediately following the dissociation. In this case we can use the expression for the kinetic energy, $E = (1/2)\mu v^2$, and substitute the relevant parameters to obtain

$$E = \tfrac{1}{2}\mu\left(\frac{L}{\tau}\right)^2, \quad (2)$$

where L is taken here as the distance the fragments must move from each other before the bond is considered broken, τ is the dissociation time (*i.e.*, transition state lifetime), and μ is the reduced mass calculated for the pseudodiatomic. The kinetic energy E represents the energy available for recoil after the enthalpy of reaction and internal energy (vibrational and rotational energy) of the products have been subtracted from the photon energy. In some situations, we will look at the maximum energy available for recoil obtained by subtracting only the reaction enthalpy from the excitation energy; the recoil energy is not partitioned into vibrational, rotational and translational motion in these cases.

Assuming the excitation process and energy partitioning in CH_2ICl to be the same as in CH_2I_2 (both dissociation channels lead to products in the D′ state), the dissociation time for CH_2ICl is in agreement with the time that would be predicted by reduced mass considerations. In addition, information about the translational and internal energy of the fragments can also be obtained with this model. Using eqn. (2) with a length parameter of 2 Å yields a translational energy in the dissociating fragments of 4278 cm^{-1} (0.53 eV) when the molecular product is ICl(G) and 9361 cm^{-1} (1.16 eV) when it

is ICl(D′), a difference of 5083 cm^{-1} or 0.63 eV. The energy separation between the G and D′ states of ICl is 6491 cm^{-1}, or 0.8 eV.[34] Thus, it appears that the majority of the excess energy available for the halogen product ICl(D′) is partitioned into kinetic energy and the remainder into internal energy of the fragments. Note that these energy comparisons are not absolute; we do not know at this time the partitioning of the internal energy in the carbene fragment for either pathway. However, of the excess 0.8 eV that should have been available as recoil for the ICl(D′) product due to the difference in the potential energies, a portion of that energy goes into vibrations and/or rotations rather than translational motion.

The 430 nm data (ICl D′ → A′) exhibits some modulation in intensity as a function of pump–probe time delay that is assigned to vibrational oscillations; this data is shown in Fig. 3a. The displayed data has been smoothed with five-point averaging and the sloping background (see Fig. 2c lower) has been subtracted. A fast Fourier transform (FFT) was performed on the data and is shown in Fig. 3b. The results show multiple frequencies that contribute to the signal; clearly the 73 cm^{-1} frequency dominates the transient and the corresponding 450 fs oscillations are evident in the data (see Fig. 3a). A longer transient with higher signal-to-noise ratio would allow a more accurate determination of the vibrational distribution observed in the D′–A′ emission. Because of the short temporal range of the data, more confidence can be placed on the higher energy peaks (73, 93, and 117 cm^{-1}). The vibrational distribution observed in the FFT is consistent with population levels $v' > 30$. Here we concentrate our analysis on the strongest feature for illustration purposes. A beat frequency of 73 cm^{-1} corresponds to a maximum near $v = 75$ for ICl(D′),[27] resulting in a vibrational energy in the fragment of 9303 cm^{-1}, or 1.15 eV. While this is a substantial amount of vibrational excitation, it is only 10% of the total energy and it is far from the dissociation energy for this state ($D_e \sim 4.17$ eV).[27] Assuming that the energy required to produce CH_2 and ICl(D′) is ~8.4 eV (similar to CH_2I_2, see Table 1), the internal energy of the CH_2 fragment can be estimated to be ~1.3 eV. We have not performed a direct spectroscopic analysis of this fragment. There were no discernible vibrational oscillations in the time-resolved fluorescence data collected at 340 nm from the CH_2ICl cell.

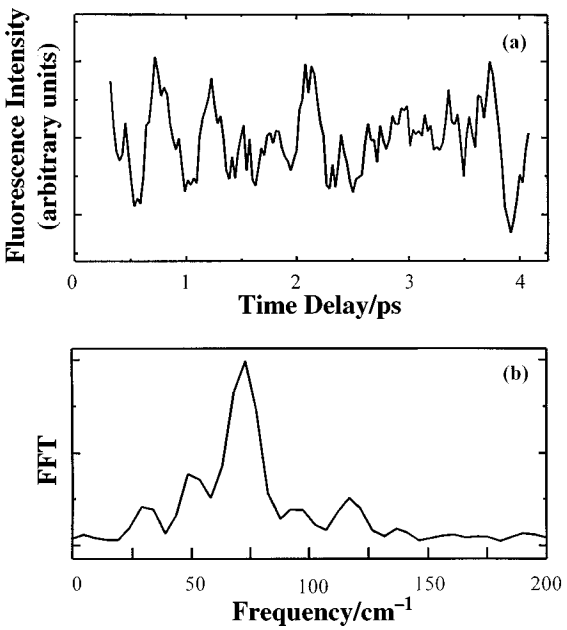

Fig. 3 (a) Transient showing the molecular dynamics following the multiphoton excitation of CH_2ICl. Note that the data shown have been averaged and had the sloped background subtracted. Vibrational oscillations are clear and other experimental transients that were taken have shown similar oscillations. (b) FFT of the transient. A wide range of vibrational excitation is obtained in this dissociation process. The major frequencies contributing to the signal are 29, 49, 73, 93 and 117 cm^{-1}.

Table 1 Thermodynamics of the dissociation reaction $CX_2Y_2 \rightarrow CX_2 + Y_2(D')$, where X = H, F or Cl and Y is Br or I[a]

Reaction	Enthalpy/cm^{-1}	eV
(i) $CH_2I_2 \rightarrow CH_2(\tilde{X}) + I_2(D')$	67588	8.38
(ii) $CH_2Br_2 \rightarrow CH_2(\tilde{X}) + Br_2(D')$	85047	10.5
(iii) $CCl_2Br_2 \rightarrow CCl_2(\tilde{X}) + Br_2(D')$	70735	8.8
(iv) $CCl_2Br_2 \rightarrow CCl_2(\tilde{A}) + Br_2(D')$	79042	9.8
(v) $CF_2Br_2 \rightarrow CF_2(\tilde{X}) + Br_2(D')$	68557	8.5
(vi) $CF_2Br_2 \rightarrow CF_2(\tilde{A}) + Br_2(D')$	88398	11.0

[a] Enthalpies of formation of reactants were taken from refs. 30 and 35 and of the products from ref. 30. The value of T_e for the D′ state of Br_2 was taken from ref. 34; singlet–triplet splittings for the carbene fragments were taken from refs. 36 and 37. Three-photon excitation at 312 nm corresponds to 96150 cm^{-1} or approximately 11.9 eV.

In addition to obtaining dissociation times, one can explore the vectorial properties of the molecular photodetachment of ICl(G) from CH_2ICl. These studies have been carried out by using pump and probe lasers polarized parallel or perpendicular to each other and by detecting the signal at 340 nm (not shown). The time-dependent anisotropy measurement is obtained with the usual formula $r(t) = (I_{\parallel} - I_{\perp})/(I_{\parallel} + 2I_{\perp})$. The $r(t)$ obtained from these transients was fit assuming a Gaussian population of rotational j levels and determining the position and FWHM of the Gaussian, using the formulation corresponding to multiphoton excitation.[15] The $r(t)$ was also fit to a thermal distribution of rotational levels because the observed rotational population closely resembled a Boltzmann distribution. The rotational population of ICl molecules is centered at approximately $j = 10$, which corresponds to a rotational temperature of approximately 170 K. This is dramatically lower than was previously observed in the I_2(f) dissociation product from CH_2I_2, which indicates that the dissociation of CH_2ICl follows a different photodetachment mechanism. This is not unexpected because the CH_2ICl molecule carries none of the transition restrictions arising from the C_{2v} symmetry of the other molecules studied.

The asymmetric dissociation of symmetric molecules has been discussed by Tamir *et al.*[38] Their conclusion, based on classical trajectory simulations and experimental observations, was that asymmetric dissociation is expected from energy-rich triatomic or pseudo-triatomic molecules of the AB_2 type. This was attributed to a larger phase space for asymmetric (*i.e.*, non-C_{2v}) dissociation. In dihalomethanes, an electronic symmetry barrier prevents the molecular detachment reaction from proceeding through the symmetric transition state, also known as the least motion pathway.[7] The lower energy pathway involves rotation of the halogen moiety, thus breaking the C_{2v} symmetry of the parent.[7]

B. Photodetachment dynamics of CX_2Br_2

Time-resolved parallel and perpendicular transients for CH_2Br_2 are shown in Fig. 4a. The signal was detected at 287 nm, corresponding to the D′ → A′ transition of Br_2.[39] The isotropic and anisotropic portions of the CH_2Br_2 signal at positive pump–probe time delays were extracted and are shown in Fig. 4b. The rotational anisotropy of the signal, $r(t)$, was fit using a Gaussian distribution of rotational levels, centered at $j_{max} = 76 \pm 7$, with a FWHM Δ_j of 170 ± 20. This corresponds to an average rotational energy in the Br_2(D′) product of 250 cm^{-1}; less than was observed in the I_2(f) fragment.[15] However, direct comparison with the I_2(D′) rotational excita-

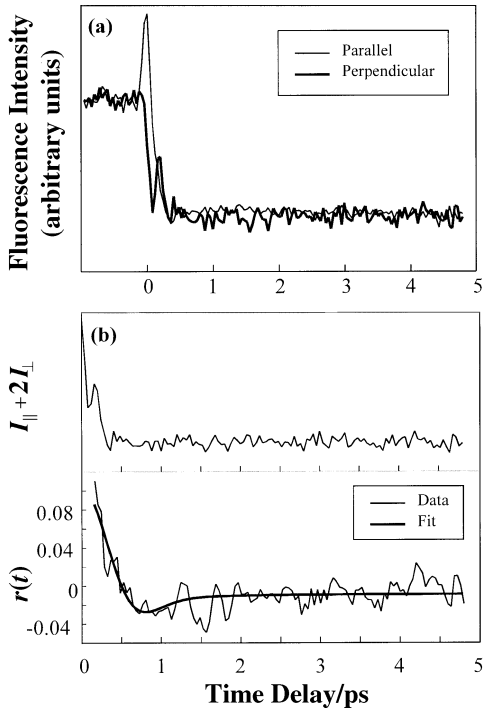

Fig. 4 (a) Experimental pump–probe transients from the CH_2Br_2 sample with the probe beam polarized parallel (thin line) and perpendicular (thick line) to the pump beam. The data was collected at 287 nm corresponding to the D′ → A′ transition of Br_2. (b) The isotropic and anisotropic contributions were extracted from the data. Vibrational modulation can not be clearly observed; however, there appears to be a single vibrational oscillation near time zero. This peak is clearly seen in the perpendicular data, but is most likely masked by the intense time zero peak in the parallel data. This vibration may be attributable to the Br–C–Br bending motion (173 cm^{-1}) or a Br–Br (D′) vibration (150 cm^{-1}). The fit to the rotational anisotropy using a Gaussian distribution yields $j_{max} = 76 \pm 7$ and $\Delta j = 170 \pm 20$, which corresponds to less rotational excitation than had been observed in the I_2(f) fragment.

tion is not possible because the rotational anisotropy at 340 nm could not be reliably analyzed.[13]

Using the fitting method outlined by Marvet *et al.*[13] resulted in a transition state lifetime of 58.6 ± 1.4 fs for the CH_2Br_2 photodetachment. Using eqn. (2), we can see why the dissociation time for CH_2Br_2 is longer than for CH_2I_2 (47 ± 3 fs). The differences in reduced mass are very small, but there are large differences in the thermodynamics of the reaction (see Table 1). Assuming that excitation at 312 nm is a three-photon process, the maximum energy available for fragment recoil from methylene iodide is about 3.6 eV, compared to 1.5 eV for methylene bromide. Note that these values do not account for internal energy; however, we assume that the partitioning will be similar in both cases because both reactions produce a carbene fragment. Therefore, a higher value for the translational energy in the iodine compound is expected. As reflected in eqn. (2), this increase in E causes the dissociation process to be faster for CH_2I_2 than for CH_2Br_2.

Molecular parameters of Br_2(D′) were used to try to fit the isotropic portion ($I_{\parallel} + 2I_{\perp}$) of the signal.[39] Unlike the CH_2I_2 transients,[9–11,13–15] vibrational modulation at positive times can not be clearly seen in this data. Analysis of several scans collected with the pump and probe lasers polarized parallel to each other did not yield consistent results either by Fourier transform or by modeling the vibrations as described previously for the CH_2I_2 data.[13,15] However, there does appear to be a single vibrational oscillation in the perpendicular data, which is probably hidden underneath time zero in the parallel data (see Fig. 4a and 4b upper). This could be due to a single Br–C–Br bend oscillation, which has a frequency of this mode in the ground state of 173 cm^{-1},[40] or to a single Br–Br vibration, where the frequency of this mode in the D′ state is 150 cm^{-1}.[39] The enhancement occurring at 185 ± 10 fs corresponds to one (perhaps two) vibrations of a mode with a frequency equivalent to 185 ± 12 cm^{-1}. Conceivably, this feature corresponds to motion of the Br atoms in the Br–C–Br bending mode during the photodetachment process.

The photodissociation dynamics of the family of compounds CH_2Y_2 where Y = Cl, Br or I have been investigated.[13] Fluorescence corresponding to the D′ → A′ transition for the respective molecular halogen products were observed and the dynamics in each case were similar with an intense time zero feature and fluorescence depletion at positive time delays. Here, we continue by exploring the photodissociation dynamics of the CX_2Br_2 family, where X = H, F or Cl. Multiphoton excitation of CH_2Br_2, CF_2Br_2 and CCl_2Br_2 using 312 nm pulses produces Br_2 in the D′ state; these spectra are shown in Fig. 5a.

We have previously reported that Br_2(D′) spectra from the dissociation of CF_2Br_2 and CH_2Br_2 at 0 °C indicate a difference in vibrational population of the halogen.[11] However, the vapor pressure of CF_2Br_2 is 314 Torr at 0 °C,[41] corresponding to a gas phase collision frequency of 2.45 × 10^9 s^{-1}. This is sufficient to cause vibrational relaxation in the observed fluorescence spectrum. In order to check this observation, spectra

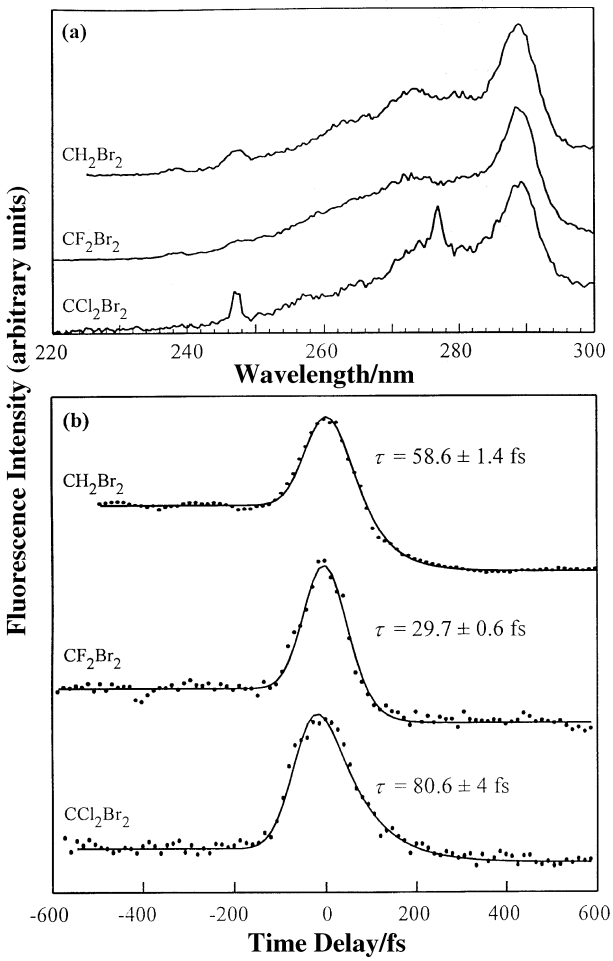

Fig. 5 (a) Spectra from the multiphoton excitation of CH_2Br_2, CF_2Br_2, and CCl_2Br_2 showing quite similar spectral features in each case. (b) Pump–probe data (dots) collected at 287 nm for these three compounds. The displayed fits correspond to dissociation times of 58.6 ± 1.4 fs, 29.7 ± 0.6 fs, and 80.6 ± 4 fs, respectively. The fluoride compound dissociates much faster than predicted by thermodynamics and the difference in the reduced mass. The transition state lifetime of the chlorine compound is on the order of what is predicted from CH_2Br_2 based on the change in the reduced mass and the difference in the reaction enthalpies.

were recorded from CH_2Br_2 and CF_2Br_2 at 0 °C and −61 °C, respectively; at these temperatures the vapor pressures are comparable (11.5 Torr for CH_2Br_2 [41] and ~12 Torr for CF_2Br_2).[42] The spectra under these conditions reveal that, in fact, the vibrational temperature in the $Br_2(D')$ product is similar whether the parent molecule is CH_2Br_2 or CF_2Br_2.[43]

Fig. 5b shows a comparison of the transition state lifetimes of CH_2Br_2, CF_2Br_2 and CCl_2Br_2. The scans were collected consecutively, with the laser intensity kept constant as far as possible to avoid apparent differences in dissociation times resulting from saturation of the transitions. Analysis of the time zero data, as before, yielded dissociation times of 58.6 ± 1.4 fs for CH_2Br_2, 80.6 ± 4 fs for CCl_2Br_2 and 29.7 ± 0.6 fs for CF_2Br_2. The dissociation time of CF_2Br_2 is significantly faster than of the other two molecules. The enthalpies of reactions for CF_2Br_2 and CCl_2Br_2 breaking into the ground state of CX_2 and $Br_2(D')$ (see (iii) and (v) in Table 1) are quite similar, so this change in transition state lifetime can not be explained by the thermodynamics of the systems involved. The energies required to produce CCl_2 and CF_2 fragments in the first excited (triplet) states were also calculated and are displayed in Table 1. In this case, the enthalpy of reaction (vi) for the fluorine species is substantially higher than the enthalpy of reaction (iv) for the chlorine species. Therefore, these alternative product channels cannot provide an explanation for the difference in dissociation time for CF_2Br_2 either. The anomalous dissociation time is possibly due to the high electron density of the fluorine atoms, which is expected to significantly affect the electronic states of the parent molecule. For this reason, the CF_2Br_2 data will not be compared with results from its analogues.

Based on reduced mass arguments, the ratio of the dissociation times of CCl_2Br_2 and CH_2Br_2 is expected to be ~2. The experimental result was 1.4. The difference can be explained by the fact that the enthalpy required to form CCl_2 and $Br_2(D')$ from CCl_2Br_2 is lower than the energy needed to produce CH_2 and $Br_2(D')$ from the dissociation of CH_2Br_2, as shown in Table 1. This difference in reaction enthalpies results in making more energy available for partitioning into fragment recoil (including internal energy as well as translational motion) in the former reaction. Thus, with an increase in the recoil energy, the dissociation time for CCl_2Br_2 is faster than anticipated based purely on the reduced mass difference (see eqn. (2) and the CH_2I_2 *vs.* CH_2Br_2 discussion). The electronics of both reactants and products are also expected to play a role in the transition state lifetime. The assumption that the dissociation can be treated as a pseudodiatomic separation with no redistribution of energy during the reaction is rather naïve in the case of CCl_2Br_2. Here the masses of the two fragments are comparable and the C–Br and C–Cl vibrational frequencies are similar. Therefore, vibrational excitation in the products may also play a role in the relative dissociation times of CCl_2Br_2 and CH_2Br_2.

Conclusions

Molecular photodetachment experiments were carried out on CH_2ICl. Product fluorescence was observed in two regions of the spectrum: 430 nm, assigned to the $D' \rightarrow A'$ transition, and 340 nm, attributed to the $G \rightarrow A$ transition. Differences in the dissociation times for the two pathways can be understood from available recoil energy arguments. Analysis of the anisotropy in the time-resolved data reveals that there is very little rotational excitation in the molecular product, being approximately equal to a thermal distribution centered at $j \approx 10$. This is very different from the results on the dissociation of CH_2X_2 in which significant rotational excitation was observed in the products and indicates a different reaction pathway. This difference is not unexpected in light of a symmetry barrier to the formation of an interhalogen bond from molecules with C_{2v} symmetry. A barrier of this type would tend to favor an asynchronous concerted mechanism of the type proposed for highly excited ion-pair states of I_2 in which the symmetry of the molecule is broken during dissociation. No such restriction exists in the case of CH_2ICl so that there is no barrier to a synchronous concerted mechanism of the type previously described.[13,15] The asynchronous concerted mechanism would be expected to produce a high degree of rotational excitation in the products; an impulsive dissociation retaining the geometry of the parent molecule would not. Therefore, it seems reasonable that the asynchronous concerted mechanism is the pathway when the parent molecule has C_{2v} symmetry and that the synchronous concerted mechanism, least motion pathway, is preferred when it does not. Based on the results presented here, this appears to be the case; however, more studies are required to confirm the generality of the observation.

The molecular detachment process was found to be slower for methylene bromide than for methylene iodide. The reason for this may be the difference in reaction enthalpy, more energy is available for recoil for CH_2I_2. Measurements of the reaction dynamics for three homodisubstituted dibromomethanes (X = H, F, Cl) yielded significantly different dissociation times: 29.7 fs for the fluorinated species, 58.6 fs for the hydrogenated species, and 80.6 fs for the chlorinated species. The difference in dissociation time between the hydrogenated and chlorinated analogues can be rationalized in terms of differences in reduced mass, reaction enthalpies, and vibrational excitation of the CX_2 product. The fluorinated compound was found to dissociate much faster than predicted by thermodynamic and reduced mass arguments.

In conclusion, the concerted elimination of halogen molecules from halogenated alkanes occurs following an ultrafast concerted process. In most cases the halogen molecules are formed in the D′ state and the differences in the transition state lifetimes can be rationalized from analyzing the available energy for recoil and the changes in the reduced mass.

Acknowledgements

This project was partially funded by an Alfred P. Sloan Research Fellowship, a Camille Dreyfus Teacher-Scholar Award and a Packard Fellowship for Science and Engineering. Additional funding was received from NSF Grant CHE-9812584.

References

1 P. J. Dyne and D. W. G. Style, *J. Chem. Soc.*, 1952, 2122.
2 D. W. G. Style and J. C. Ward, *J. Chem. Soc.*, 1952, 2125.
3 M. Kawasaki, S. J. Lee and R. Bersohn, *J. Chem. Phys.*, 1975, **63**, 809.
4 G. Black, *Research on High Energy Storage for Laser Amplifiers*, MP76-107, Stanford Research Institute, Stanford, CA, 1976.
5 H. Okabe, M. Kawasaki and Y. Tanaka, *J. Chem. Phys.*, 1980, **73**, 6162.
6 W. H. Pence, S. L. Baughcum and S. R. Leone, *J. Phys. Chem.*, 1981, **85**, 3844.
7 S. R. Cain, R. Hoffmann and E. R. Grant, *J. Phys. Chem.*, 1981, **85**, 4046.
8 C. Fotakis, M. Martin and R. J. Donovan, *J. Chem. Soc., Faraday Trans.*, 1982, **78**, 1363.
9 U. Marvet and M. Dantus, in *Femtosecond Dynamics of Concerted Elimination Processes*, ed. M. Chergui, World Scientific, Singapore, 1996, p. 134.
10 U. Marvet and M. Dantus, *Chem. Phys. Lett.*, 1996, **256**, 57.
11 Q. Zhang, U. Marvet and M. Dantus, *J. Chem. Soc., Faraday Discuss.*, 1997, **108**, 63.
12 I. Pastirk, E. J. Brown, Q. Zhang and M. Dantus, *J. Chem. Phys.*, 1998, **108**, 4375.
13 U. Marvet, Q. Zhang, E. J. Brown and M. Dantus, *J. Chem. Phys.*, 1998, **109**, 4415.
14 U. Marvet, Q. Zhang and M. Dantus, *J. Phys. Chem.*, 1998, **102**, 4111.

15 Q. Zhang, U. Marvet and M. Dantus, *J. Chem. Phys.*, 1998, **109**, 4428.
16 W. Radloff, P. Farmanara, V. Stert, E. Schreiber and J. R. Huber, *Chem. Phys. Lett.*, 1998, **291**, 173.
17 E. A. J. Wannenmacher, P. Felder and J. R. Huber, *J. Chem. Phys.*, 1991, **95**, 986.
18 G. Baum, P. Felder and J. R. Huber, *J. Chem. Phys.*, 1993, **98**, 1999.
19 K. Bergmann, R. T. Carter, G. E. Hall and J. R. Huber, *J. Chem. Phys.*, 1998, **109**, 474.
20 B. J. Schwartz, J. C. King, J. Z. Zhang and C. B. Harris, *Chem. Phys. Lett.*, 1993, **203**, 503.
21 A. N. Tarnovsky, J. L. Alvarez, A. P. Yartsev, V. Sundstrom and E. Akesson, *Chem. Phys. Lett.*, 1999, **312**, 121.
22 G. Maier and H. P. Reisenauer, *Angew. Chem. Int. Ed. Engl.*, 1986, **25**, 819.
23 W. M. Kwok and D. L. Phillips, *Chem. Phys. Lett.*, 1995, **325**, 260.
24 W. M. Kwok and D. L. Phillips, *J. Chem. Phys.*, 1996, **104**, 2529.
25 F. Duschek, M. Schmitt, P. Vogt, A. Materny and W. Kiefer, *J. Raman Spectrosc.*, 1997, **28**, 445.
26 J. C. D. Brand, D. Bussieres, A. R. Hoy and S. M. Jaywant, *Chem. Phys. Lett.*, 1984, **109**, 101.
27 J. D. Spivey, J. G. Ashmore and J. Tellinghuisen, *Chem. Phys. Lett.*, 1984, **109**, 456.
28 J. B. Hudson, L. J. Sauls, P. S. Tellinghuisen and J. Tellinghuisen, *J. Mol. Spectrosc.*, 1991, **148**, 50.
29 G. V. Calder and W. F. Giauque, *J. Phys. Chem.*, 1965, **69**, 2443.
30 NIST Chemistry WebBook (Online), in 'NIST Standard Reference Database Number 69', National Institute of Standards and Technology, ed. W. G. Mallard and P. J. Linstrom, http://webbook.nist.gov, November 24, 1998.
31 D. R. Lide, in *Handbook of Chemistry and Physics*, CRC Press, Boca Raton, FL, 1993–4.
32 M. J. Rosker, M. Dantus and A. H. Zewail, *J. Chem. Phys.*, 1998, **89**, 6113.
33 M. Dantus, M. J. Rosker and A. H. Zewail, *J. Chem. Phys.*, 1988, **89**, 6128.
34 J. C. D. Brand and A. R. Hoy, *Appl. Spectrosc. Rev.*, 1987, **23**, 285.
35 S. A. Kudchadker and A. P. Kudchadker, *J. Phys. Chem. Ref. Data*, 1975, **4**, 457.
36 G. L. Gutsev and T. Ziegler, *J. Phys. Chem.*, 1991, **95**, 7220.
37 S. Koda, *Chem. Phys.*, 1982, **66**, 383.
38 M. Tamir, U. Halavee and R. D. Levine, *Chem. Phys. Lett.*, 1974, **25**, 38.
39 A. Sur and J. Tellinghuisen, *J. Mol. Spectrosc.*, 1981, **88**, 323.
40 B. Schrader and W. Meier, in *DMS Raman/IR Atlas of Organic Compounds*, Verlag Chemie GmbH, Weinheim. 1974.
41 D. R. Lide, in *Handbook of Chemistry and Physics*, CRC Press, Boca Raton, FL, 1996–7.
42 Calculated using data from ref. 41 and a modified Clausius–Clapeyron of the form $\log(p) = -0.2185A/T + B$ (R. C. Weast, in *Handbook of Chemistry and Physics*, The Chemical Rubber Co., Cleveland, OH, 1972–3).
43 U. Marvet, PhD Thesis, Michigan State University, East Lansing, MI, 1998.

Paper a908173i